Biochemical and Biophysical Research Communications 452 (2014) 593–599

Contents lists available at ScienceDirect

Biochemical and Biophysical Research Communications

journal homepage: www.elsevier.com/locate/ybbrc

High-temperature calcined fullerene nanowhiskers as well as long needle-like multi-wall carbon nanotubes have abilities to induce NLRP3-mediated IL-1β secretion

Hongyan Cui [a], Weijia Wu [a], Keiichiro Okuhira [a], Kun'ichi Miyazawa [b], Takayuki Hattori [a], Kimie Sai [a], Mikihiko Naito [a], Kazuhiro Suzuki [a], Tetsuji Nishimura [a], Yoshimitsu Sakamoto [c], Akio Ogata [c], Tomokazu Maeno [c], Akiko Inomata [c], Dai Nakae [c], Akihiko Hirose [a], Tomoko Nishimaki-Mogami [a,*]

[a] Division of Biochemistry and Metabolism, Division of Biochemistry and Molecular Biology, Division of Environmental Chemistry, Division of Risk Assessment, and Biological Safety Research Center, National Institute of Health Sciences, Tokyo 158-8501, Japan
[b] Fullerene Engineering Group, Materials Processing Unit, National Institute for Materials Science, Tsukuba, Ibaraki 305-0044, Japan
[c] Department of Environmental Health and Toxicology, Tokyo Metropolitan Institute of Public Health, Tokyo 169-0073, Japan

ARTICLE INFO

Article history:
Received 4 August 2014
Available online 30 August 2014

Keywords:
Carbon nanotubes
Fullerene nanowhiskers
IL-1β
NLRP3

ABSTRACT

Because multi-wall carbon nanotubes (MWCNTs) have asbestos-like shape and size, concerns about their pathogenicity have been raised. Contaminated metals of MWCNTs may also be responsible for their toxicity. In this study, we employed high-temperature calcined fullerene nanowhiskers (HTCFNWs), which are needle-like nanofibers composed of amorphous carbon having similar sizes to MWCNTs but neither metal impurities nor tubular structures, and investigated their ability to induce production a major pro-inflammatory cytokine IL-1β via the Nod-like receptor pyrin domain containing 3 (NLRP3)-containing flammasome-mediated mechanism. When exposed to THP-1 macrophages, long-HTCFNW exhibited robust IL-1β production as long and needle-like MWCNTs did, but short-HTCFNW caused very small effect. IL-1β release induced by long-HTCFNW as well as by long, needle-like MWCNTs was abolished by a caspase-1 inhibitor or siRNA-knockdown of NLRP3, indicating that NLRP3-inflammasome-mediated IL-1β production by these carbon nanofibers. Our findings indicate that the needle-like shape and length, but neither metal impurities nor tubular structures of MWCNTs were critical to robust NLRP3 activation.

1. Introduction

Carbon nanotubes (CNTs) are increasingly being used in various industrial fields because of their unique electronic and mechanical properties. However, these unique physicochemical properties, especially the asbestos-like shape and size with a high-aspect ratio, are currently of great concern with respect to the environment and human health [1]. A variety of multiwall carbon nanotubes (MWCNTs) and single-wall carbon nanotubes have been produced, and some of these materials have been shown to cause mesothelioma after injection into the abdominal cavities of p53+/− mice [2] or the scrotum of wild-type rats [3]. Inflammatory cell recruitment and granulomas [4] and elevated mRNA expression of pro-inflammatory cytokines and chemokines in peritoneal cells [5] were induced by MWCNTs injected into the abdominal cavities of mice. Pulmonary exposed MWCNTs were shown to reach subpleural tissue and macrophages in mice and rats and to induce fibrosis, inflammation, allergic immune responses [6–8] and mesothelial proliferation [9]. Abundant inflammatory cell infiltration and increased pro-inflammatory cytokine levels in the pleural cavity were also observed [9,10].

IL-1β is an important proinflammatory cytokine that is generated at sites of injury, infection, or immunological challenge to recruit immune cells [11]. It is very likely that IL-1β plays a major role in MWCNT-induced inflammation or immune responses. Recent studies have revealed that IL-1β maturation and release are controlled by a large multiprotein complex, called the inflammasome [11]. In particular, the inflammasome containing the Nod-like receptor (NLR)-family protein 3, NLRP3, can be activated

Abbreviations: MWCNTs, multi-wall carbon nanotubes; HTCFNWs, high-temperature calcined fullerene nanowhiskers; NLRP3, Nod-like receptor pyrin domain containing 3; CNTs, carbon nanotubes; SSC, side scatter; FSC, forward scatter.

* Corresponding author. Address: Division of Biochemistry and Metabolism, National Institute of Health Sciences, Kamiyoga 1-18-1, Setagaya-ku, Tokyo 158-8501, Japan. Fax: +81 3 3707 6950.
E-mail address: mogami@nihs.go.jp (T. Nishimaki-Mogami).

http://dx.doi.org/10.1016/j.bbrc.2014.08.118
0006-291X/

by a variety of danger signals or phagocytosed crystals and aggregated proteins and has been implicated in several chronic inflammatory diseases [11,12]. Certain MWCNTs have been shown to induce NLRP3-mediated IL-1β secretion [13,14]. Various MWCNTs with different physicochemical properties, including length, diameter, and contaminant metals, are produced. However, factors that are critical to inducing NLRP3 activation and/or IL-1β production remain unclear.

Shape and size of MWCNTs similar to asbestos have been implicated in their toxicity. In addition, several studies have suggested that metal contamination, which is derived from catalysts used in the synthesis of CNTs, is responsible for cytotoxicity and genotoxicity of MWCNTs [15–18] and for the redox-dependent response of macrophages [19], although this suggestion remains controversial [4,20].

In this study, we employed high-temperature calcined fullerene nanowhiskers (HTCFNWs), which are amorphous carbon nanofibers and have a needle-like morphology with similar length to MWCNTs [21]. Notably, HTCFNWs do not contain metal impurities, because they are produced from fullerene nanowhiskers by heating in vacuum [21]. Fullerene nanowhiskers are thin, single crystal nanofibers composed of C_{60} fullerene molecules that are bound via van der Waals forces [22]. We investigated the ability of long or short HTCFNW, which did not contain tubular structures and metal impurities, and various MWCNTs with different physical properties to induce IL-1β secretion, and sought to identify factors required for inducing NLRP3-mediated IL-1β release.

2. Materials and methods

2.1. Materials

We used three types of MWCNT grown in the vapor phase (Fig. 1A): MWCNT-M was provided by Nanocarbon Technologies Co., Ltd. (Tokyo, Japan). MWCNT-SD1 and MWCNT-SD2 were by Showa-Denko Co., Ltd. (Tokyo, Japan). HTCFNW-L and -S were prepared by heating fullerene nanowhiskers at 900 °C in vacuum [21]. Fullerene nanowhiskers were synthesized from C_{60} fullerene by a liquid–liquid interfacial precipitation method [23]. The size distribution of MWCNTs and HTCFNWs was determined by scanning electron microscopy. Fe contents were determined by a collision type inductively coupled plasma mass spectrometer as described [2].

2.2. Preparation of MWCNT and HTCFNW dispersions

MWCNTs were suspended in phosphate-buffered saline (PBS) containing 0.5% Tween-20 (or Tween-80) at a concentration of 0.5 mg/mL, sonicated with a bath-type sonicator (BRNSON 1200) for 1 min × 3, and then diluted with PBS to a concentration of 0.2 mg/mL. The suspension of carbon nanotubes was homogenized by passing through a 30G needle. HTCFNWs (0.5 mg/mL) were dispersed in 0.1% Tween 80.

2.3. Cell culture and treatment of cells with HTCFNWs and MWCNTs

THP-1 cells (obtained from American Type Culture Collection (ATCC), Manassas, VA) were maintained in RPM-1 medium containing 10% fetal bovine serum (FBS). Cells were plated at a density of 3.5×10^5 cells in 24 well plates, differentiated for 72 h with 0.3 μM PMA, and further incubated for 24 h without PMA. The cells were treated for 6 h with carbon nanomaterials or the indicated stimuli. As indicated, 10 μM of caspase-1 inhibitor z-YVAD-fmk (Calbiochem), 0.2 μM cytochalasin D (Sigma), 130 mM KCl, 3 mM ATP, or 3.4 μM nigericin (Sigma) was added to the incubation medium. Cell extract and the medium supernatant were collected for analysis of their cytokine content. Cell viability was assessed by release of LDH to the medium (with a Cytotoxicity Detection Kit Plus (Roche)) or by the Tetracolor one cell proliferation assay, which detects vital mitochondrial function (Seikagaku Kogyo Ltd., Tokyo).

2.4. Analysis of IL-1β secretion

IL-1β in the medium supernatant was analyzed by the Milliplex immunoassay (Merck Co., Ltd.) according to the manufacturer's protocol or by Western blotting.

2.5. Flow cytometry analysis to detect cellular uptake of MWCNTs and HTCFNWs

PMA-differentiated THP-1 cells were exposed to MWCNTs or HTCFNWs for 20 h. The cells were washed, trypsinized, suspended in PBS containing 10% FBS, and filtered through 100 μm nylon mesh. The uptake of carbon nanofibers was determined by flow cytometry (FACSCalibur™; BD Biosciences) measuring side scatter (SSC) and forward scatter (FSC) of 10,000 counts.

2.6. Western blotting

Cells were extracted with RIPA containing the protease inhibitor cocktail set III (1:100) (Calbiochem). The culture medium supernatant was concentrated with a Microkon Ultracel YM-10 (10 kDa cut-off; Millipore, Bedford, MA) or Amicon Ultra-3K (3 kDa cut-off; Millipore, Bedford, MA). Cell extract and medium samples were analyzed by polyacrylamide gel electrophoresis followed by transfer to an Immobilon-P Transfer Membrane (Millipore). Anti IL-1β antibody (sc-7884), anti-caspase-1 P-10 antibody (sc-515) (Santa Cruz Biotechnology, Inc), and anti β-actin antibody (Sigma) were used. The immunoreactive proteins were visualized using ECL (GE Healthcare, Piscataway, NJ) or a SuperSignal West Femto Substrate kit (Thermo Scientific, Rockford, IL), and light emission was quantified with a LAS-3000 lumino-image analyzer (Fuji, Tokyo, Japan).

2.7. NLRP3 knockdown by RNA interference

THP-1 cells were plated at a density of 1.75×10^6 cells in 12 well plates and were differentiated for 72 h with 0.3 μM PMA. Cells were transiently transfected with gene-specific StealthTM Select RNAi or Stealth RNAi negative control (Invitrogen, Carlsbad, CA) using lipofectamine RNAi MAX reagent (Invitrogen) for 24 h. The Stealth RNAi sequences used were human NLRP3 sense1 (5′-AACCCAGGCACACUCCUCCUGUAGC-3′), antisense1 (5′-GCUACAG GAGGAGUGUGCCUGGGUU-3′); sense2 (5′-UUCUGUUGCUGGCUU CCUCAGCACA-3′), antisense2 (5′-UGUGCUGAGGAAGCCAGCAACA GAA-3′); sense3 (5′-UCCUGUGCUACUCCAGUAACCCAGG-3′), and antisense3 (5′-CCUGGGUUACUGGAGUAGCACAGGA-3′).

2.8. RNA extraction and quantitative real-time RT-PCR

Total RNA was extracted with an RNeasy Mini Kit using on-column deoxyribonuclease digestion to eliminate genomic DNA contamination according to the manufacturer's instructions (Qiagen, Valencia, CA). Quantitative real-time RT-PCR was performed with an ABI Prism 7300 sequence detection system using the TaqMan one-step RT-PCR Master Mix Reagent Kit (Applied Biosystems, Foster City, CA) with TaqMan probes/primers as follows: human NLRP3, forward: 5′-TGAGCCTCAACAAACGCTACA-3′; reverse: 5′-CTTGCCGATGGCCAGAAG -3′; probe: 5′-FAM-CTGCGTCTCATCAAG GAGCACCGG-BHQ-3′. 18S rRNA (Applied Biosystems). Expression

data were normalized to 18S rRNA levels, and are presented as the fold difference between treated and untreated cells.

2.9. Statistical analysis

Data were analyzed by ANOVA followed by the Student–Newman–Keuls method. Statistical significance was established at the $P < 0.05$ level.

3. Results

3.1. HTCFNWs and various MWCNTs display different abilities to induce IL-1β production

HTCFNWs are the fullerene nanowhiskers heat-treated in vacuum at 900 °C and are composed of amorphous carbon [21]. Two types of HTCFNWs with different lengths and diameters (Fig. 1A) were examined for their ability to induce IL-1β production compared with MWCNT-SD1 in the human macrophage-like cell line THP-1 cells. As shown in Fig. 1B *left*, long HTCFNWs (HTCFNW-L) caused robust IL-1β production in a dose-dependent manner, which corresponded to ca. 30% of the MWCNT-SD1-induced stimulation at the same concentration. Short HTCFNWs (HTCFNW-S) had a very small but significant and phagocytosis-dependent effect (Fig. 1B *right*). We also investigated the ability of various MWCNTs with different physical properties (Fig. 1A) to stimulate IL-1β production. MWCNT-M, -SD1, or -SD2 dose-dependently induced IL-1β secretion into the medium (Fig. 1C). IL-1β production induced by MWCNT-M or -SD1 was almost completely inhibited by pretreating cells with the phagocytosis inhibitor cytochalasin D that impairs the actin filament assembly (Fig. 1D), indicating that the uptake of MWCNTs into cells is required for stimulation of IL-1β production.

These findings clearly show that MWCNTs with various physical properties exhibit different abilities to induce IL-1β production, and HTCFNWs without impurities exhibited a comparable effect to MWCNTs.

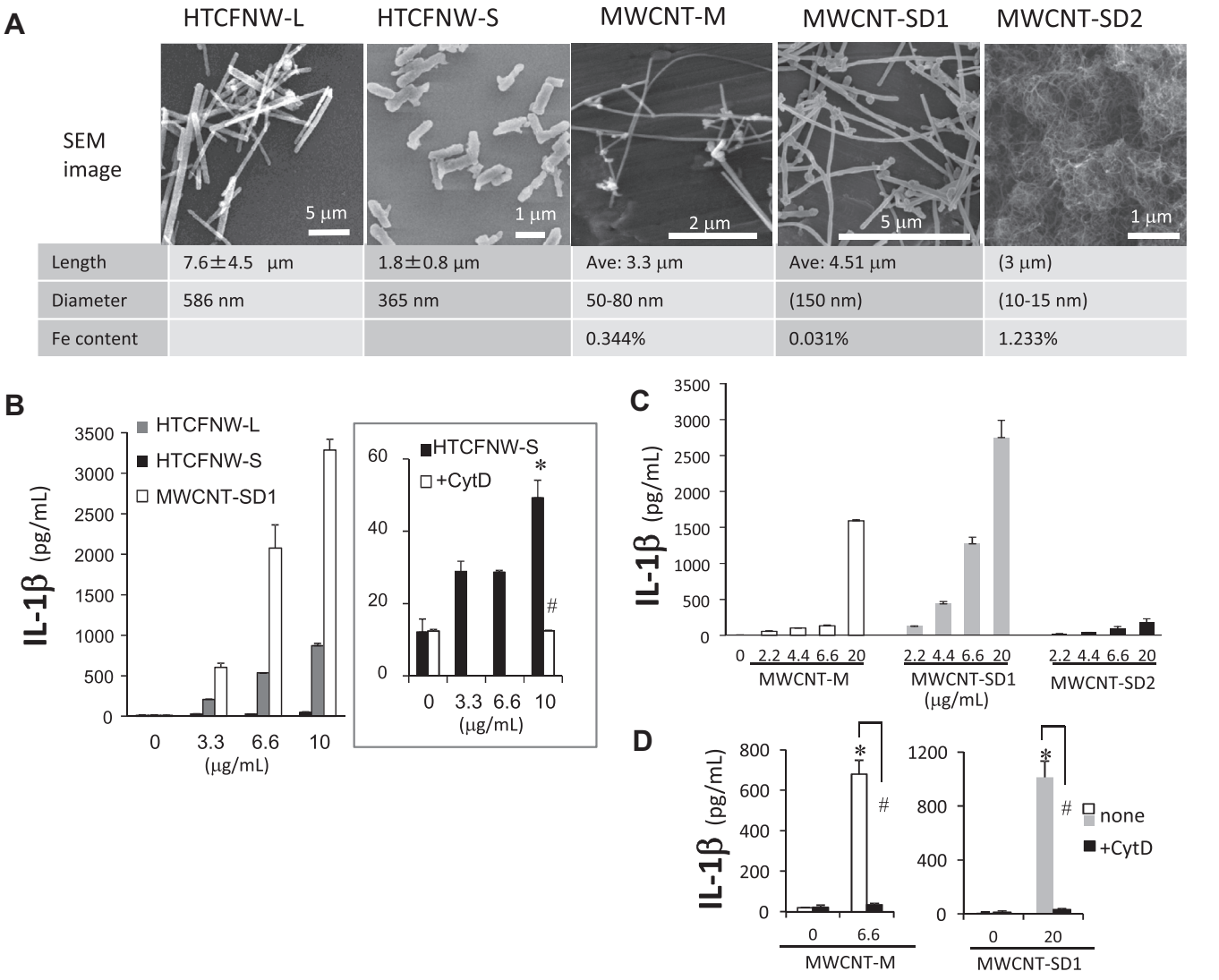

Fig. 1. HTCFNWs as well as long-, needle-like MWCNTs have abilities to induce IL-1β production. (A) Specification of the HTCFNWs and MWCNTs used in this study. Characteristics in parenthesis were provided by manufacturers. (B–D) THP-1 cells were stimulated for 6 h with the indicated amount (μg/mL of media) of HTCFNW-L, -S, and MWCNT-SD1 dispersed in Tween 80 (final concentration, 0.002%), or MWCNT-M, -SD1, and -SD2 dispersed in Tween 20 (final concentration, 0.002%) (C, D). Phagocytosis was inhibited by treating cells with cytochalasin D (0.2 μM) for 30 min before stimulation. IL-1β in the medium was analyzed by the Milliplex immunoassay. Data represent means ± S.D ($n = 2$). Significant difference from vehicle control (*) or between cytochalasin D-untreated and -treated cells (#). A vertical axis for a HTCFNW-S graph was expanded in the right panel (B).

Internalization of nanofibers by cells was evaluated with the SSC value from flow cytometry. The SSC is directly related to cell granularity and is used as a measurement of the uptake of particles or nanofibers [24,25]. Exposure of cells to MWCNT-SD1 or MWCNT-M resulted in increases in the SSC values (Fig. 2A and B), which were inhibited by the phagocytosis inhibitor cytochalasin D (Fig. 2C). MWCNT-SD2, with an agglomerate morphology, had no effect. HTCFNW-L and -S caused similar levels of SSC increase (Fig. 2D).

3.2. HTCFNW as well as MWCNTs promote caspase-1 cleavage via NLRP3 activation

The mature form of IL-1β is cleaved from the pro-IL-1β precursor by caspase-1. As shown in Fig. 3A, MWCNT-SD1 induced a potent, dose-responsive release of mature IL-1β (p17) to the medium, which was accompanied by an increase in the active caspase-1 fragment (p10). As a positive control, we confirmed that the bacterial ionophore nigericin promoted caspase-1 cleavage and IL-1β maturation. Furthermore, IL-1β secretion induced by MWCNT-M was completely inhibited by the caspase-1-inhibitor zYVAD-fmk (Fig. 3B). IL-1β release induced by MWCNT-SD1 (Fig. 3C) and HTCFNW-L (Fig. 3D) was similarly repressed by zYVAD-fmk. These findings indicate that HTCFNW-L, as well as needle-like MWCNTs, induces activation of caspase-1.

Caspase-1 is auto-activated by a signal within the multiprotein complex known as the "inflammasome" [11]. We examined whether the NLRP3-containing inflammasome is involved in MWCNT-induced IL-1β production. NLRP3 inflammasome activation is known to require potassium (K+) efflux [11]. As reported that asbestos-induced secretion of mature IL-1β was repressed by a high concentration of KCl added to the medium to inhibit K+ efflux [26], MWCNT-M-induced IL-1β secretion was blocked by KCl in the medium (Fig. 3B).

To test the role of NLRP3, siRNA knockdown of NLRP3 was performed. In THP-1 cells, three different siRNAs against NLRP3 effectively reduced NLRP3 mRNA expression (Fig. 4A). MWCNT-M-induced IL-1β secretion, determined by immunoassay, was effectively reduced by three different NLRP3 siRNAs (Fig. 4C). This reduction was accompanied by reductions of the active form of capsase-1 (p10) and cleaved IL-1β into the medium (Fig. 4B). Il-1β secretion elicited by MWCNT-SD1 or HTCFNW-L was also diminished by the NLRP3 siRNA (Fig. 4D and E). These findings clearly demonstrate that NLRP3 is involved in IL-1β maturation induced by HTCFNW-L as well as needle-like MWCNTs.

4. Discussion

In this study, we showed that fullerene-derived HTCFNWs and certain MWCNTs, with a long, needle like morphology potently

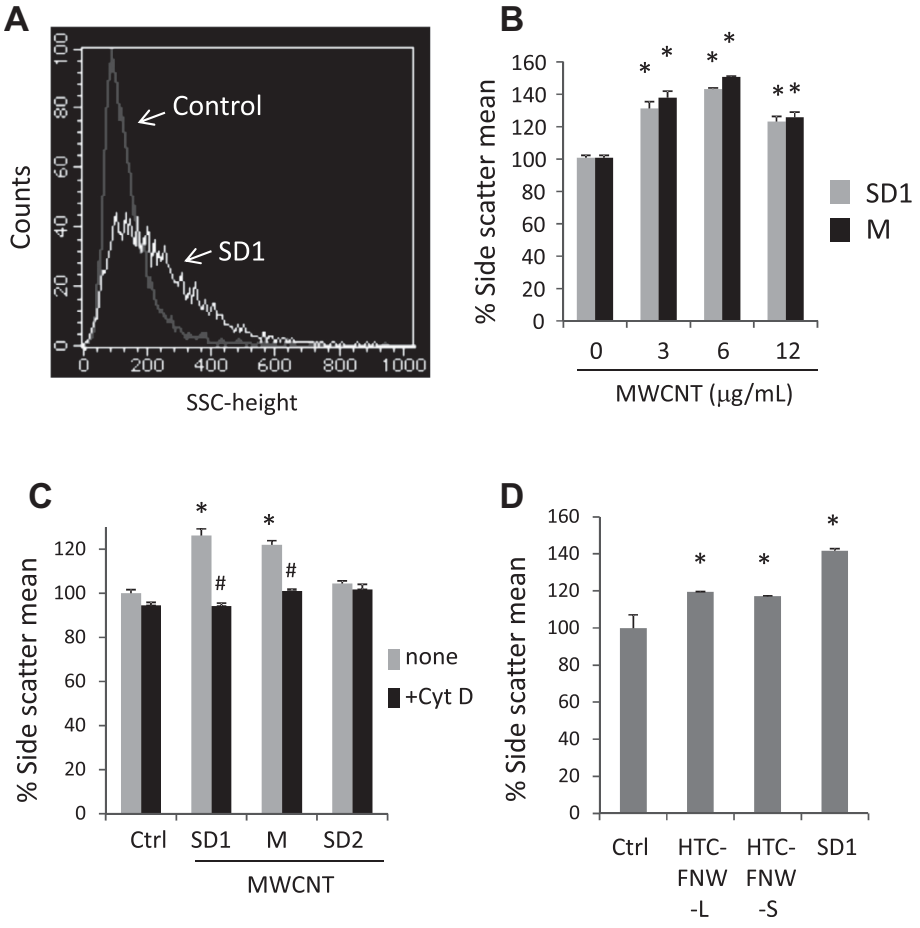

Fig. 2. Flow cytometry analysis shows cell internalization of MWCNTs and HTCFNWs. THP-1 cells were treated with or without cytochalasin D (0.2 μM) for 30 min and were then exposed to the indicated concentration of MWCNT-SD1, -SD2, -M, HTCFNW-L or -S dispersed in Tween 80 (final concentration, 0.002%) for 20 h. The cells were trypsinized and analyzed by flow cytometry. (A) Representative histogram shows the cell count vs side scatter (SSC) for cells treated without (gray line) or with MWCNT-SD1 (6 μg/mL) (white line). (B–D) Mean of the SSC value of cells treated without or with increasing concentrations of MWCNT-SD1 or -M (B), or 6 μg/mL of MWCNTs or HTCFNWs (C, D). Uptake was detectable as an increase in cell number with higher SSC. Data represent means ± S.D (n = 2 or 3). Significant difference from vehicle control (*) or between cytochalasin D-untreated and -treated cells (#).

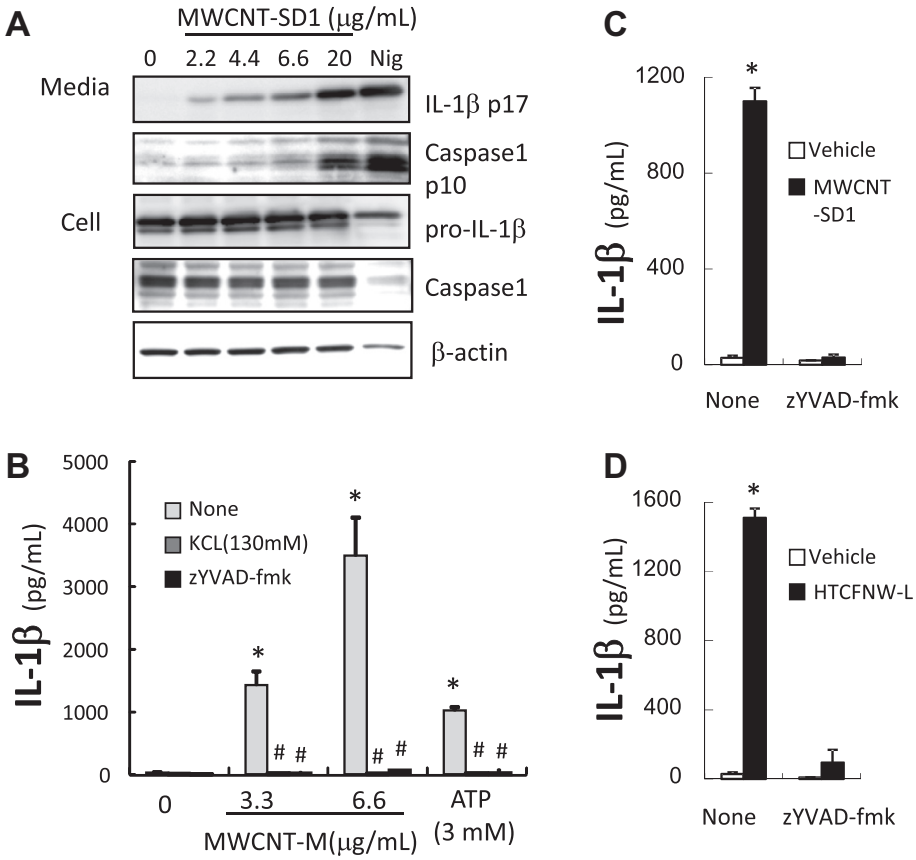

Fig. 3. MWCNT- and HTCFNW-induced IL-1β secretion accompanies caspase-1 cleavage and is repressed by extracellular KCl (130 mM) or a caspase-1 inhibitor. (A) THP-1 cells were stimulated for 6 h with the indicated amount (μg/mL of media) of MWCNT-SD1 dispersed in 0.002% Tween 20 or nigericin (Nig) (3.4 μM). The cell lysate and medium were analyzed by immunoblotting. (B–D) THP-1 cells were treated for 6 h with MWCNT-M or ATP (3 mM) (B), or MWCNT-SD1 (10 μg/mL) (C) and HTCFNW-L (10 μg/mL) (D) dispersed in 0.002% Tween 80 in the presence or absence of 130 mM KCl or the caspase-1 inhibitor zYVAD-fmk (10 μM). IL-1β in the medium was analyzed by the Milliplex immunoassay. Data represent means ± S.D ($n = 2$). Significant difference from vehicle control (*) or between inhibitor-untreated and -treated cells (#).

induce proinflammatory cytokine IL-1β production in human macrophage-like THP-1 cells (Fig. 1). Prominent IL-1β release by these nanomaterials was sensitive to the phagocytosis inhibitor cytochalasin D (Fig. 1B) and was accompanied by increases in cellular SSC values related to particle internalization (Fig. 2). Notably, HTCFNW-L and -S produced a potent and faint IL-1β release, respectively (Fig. 1C), whereas both fibers caused similar changes in the cellular SSC level (Fig. 2D). These findings clearly indicate that the needle-like shape and length of carbon nanofibers are critical to inducing IL-1β release after being taken up by cells.

The prominent IL-1β production by MWCNT-M, MWCNT-SD1, and HTCFNW-L was repressed by a high concentration of potassium or caspase-1 inhibitor and was accompanied by an increase in the active-form of caspase-1 release. Knockdown of NLRP3 by specific siRNAs diminished IL-1β production induced by these nanofibers, indicating that the NLRP3-containing inflammasome is involved in IL-1β release induced by fullerene-derived HTCFNW-L as well as long, needle-like MWCNTs.

NLRP3 is known to be activated by a variety of danger signals, including endogenous crystals of monosodium urate and cholesterol, exogenous silica crystals, aluminum salts, carbon nanotubes, and bacterial toxins, and the complex plays a critical role in IL-1β-mediated pathology [11,12]. Although the mechanism of NLRP3 activation is still unclear, potassium efflux, ROS generation, and lysosome destabilization have been implicated in NLRP3-inflammasome activation [11,12]. Changes in the redox environment have been suggested to modulate the NLRP3 inflammasome activation potential [27]. Our findings indicate that the ability of HTCFNW-L to induce NLRP3-mediated IL-1β release is comparable to that of MWCNT-M and -SD1. HTCFNWs have a needle-like morphology and similar size to MWCNT-M and -SD1. However, unlike MWCNTs, HTCFNWs contain no tubular structures or metal impurities such as Fe or Ni. Previous studies have suggested that metal contamination of CNTs is responsible for their toxicity [16–18] and cellular redox-response [19]. Importantly, HTCFNW-L and -S, which were synthesized from pure fullerene by liquid–liquid interfacial precipitation methods [23] followed by sintering with heat-treatment, contain no metal impurities. Thus, our findings clearly demonstrate that long, needle-like structures of MWCNTs and HTCFNW-L, but not metal contaminants, are required for NLRP3 inflammasome activation leading to the resulting IL-1β release.

The NLPR3-inflamasome has been implicated in several chronic inflammatory diseases such as metabolic syndrome, inflammatory bowel disease, atherosclerosis, and Alzheimer disease, as well as in regulating antimicrobial and mucosal immune responses [12,28]. Our findings raise concerns that MWCNTs may affect these diseases and responses through stimulating NLRP3-mediated IL-1β production.

In conclusion, we have shown for the first time that fullerene-derived HTCFNW-L as well as MWCNTs induces IL-1β release in an NLRP3-mediated process. Our findings indicate that the needle-like shape and length of MWCNTs, but not metal impurities or tubular structures, play a critical role in robust NLRP3 activation, which is closely implicated in chronic inflammatory diseases.

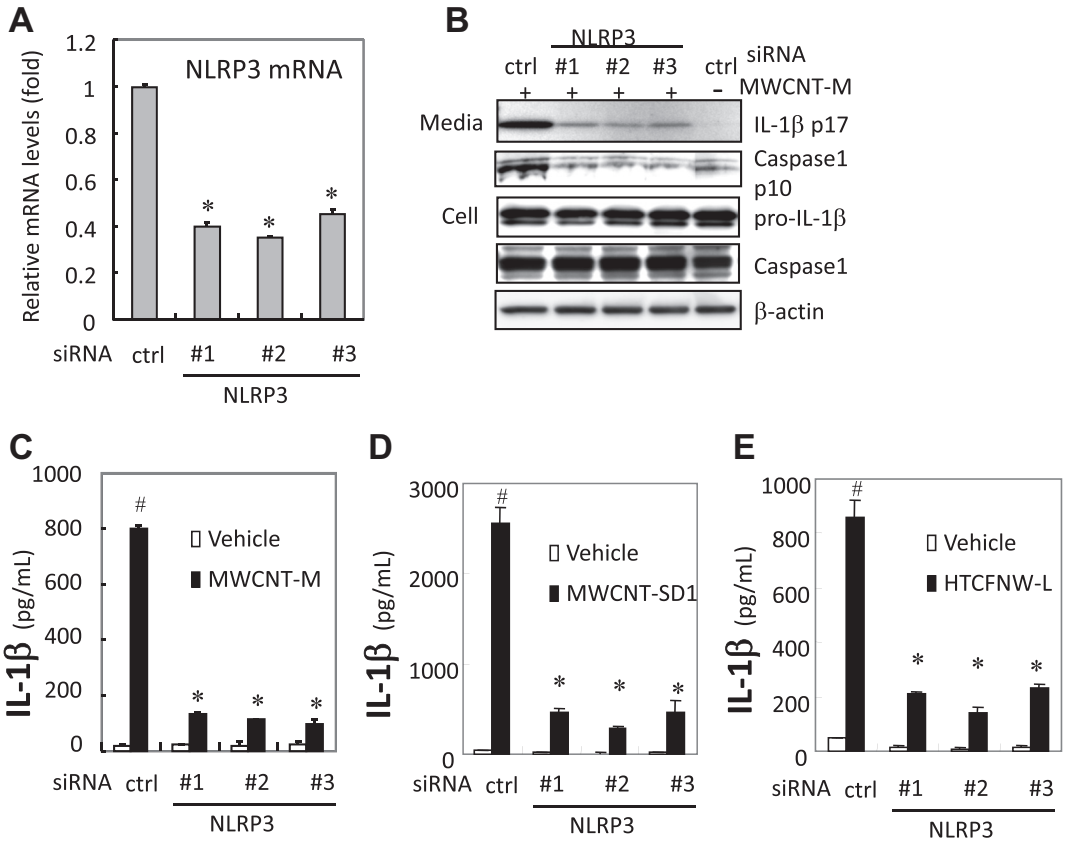

Fig. 4. Knockdown of NLRP3 diminishes MWCNT- and HTCFNW-elicited IL-1β secretion. THP-1 cells were transfected with either siRNA against three different sequences of NLRP3 (#1–3) or a negative control siRNA. After 24 h, cells were treated with MWCNT-M (6.6 μg/mL) (B, C), MWCNT-SD1 (10 μg/mL) (D) dispersed in 0.002% Tween 20, or HTCFNW-L (10 μg/mL) in Tween 80 (E) for 6 h. (A) NLRP3 mRNA levels were measured by quantitative real-time RT-PCR analysis normalized with the 18S rRNA. (B) IL-1β (p17) and caspase-1 (p10) in the medium and pro-IL-1β and caspase-1 in the cell lysate were analyzed by immunoblotting. (C–E) IL-1β in the medium was analyzed by the Milliplex immunoassay. Data represent means ± S.D. (n = 3 or 2). Significant difference from vehicle-treated control (#) or control siRNA-transfected cells (*).

Acknowledgments

This work was supported by a Health, Labor, and Welfare Sciences Research Grant (H21-kagaku-ippan-008, H24-kagaku-shitei-009, H26-kagaku-ippan-004), and in part by JSPS KAKENHI Grant Number 23590164.

References

[1] K. Donaldson, R. Aitken, L. Tran, V. Stone, R. Duffin, G. Forrest, A. Alexander, Carbon nanotubes: a review of their properties in relation to pulmonary toxicology and workplace safety, Toxicol. Sci. 92 (2006) 5–22.
[2] A. Takagi, A. Hirose, T. Nishimura, N. Fukumori, A. Ogata, N. Ohashi, S. Kitajima, J. Kanno, Induction of mesothelioma in p53+/- mouse by intraperitoneal application of multi-wall carbon nanotube, J. Toxicol. Sci. 33 (2008) 105–116.
[3] Y. Sakamoto, D. Nakae, N. Fukumori, K. Tayama, A. Maekawa, K. Imai, A. Hirose, T. Nishimura, N. Ohashi, A. Ogata, Induction of mesothelioma by a single intrascrotal administration of multi-wall carbon nanotube in intact male Fischer 344 rats, J. Toxicol. Sci. 34 (2009) 65–76.
[4] C.A. Poland, R. Duffin, I. Kinloch, A. Maynard, W.A. Wallace, A. Seaton, V. Stone, S. Brown, W. Macnee, K. Donaldson, Carbon nanotubes introduced into the abdominal cavity of mice show asbestos-like pathogenicity in a pilot study, Nat. Nanotechnol. 3 (2008) 423–428.
[5] A. Yamaguchi, T. Fujitani, K. Ohyama, D. Nakae, A. Hirose, T. Nishimura, A. Ogata, Effects of sustained stimulation with multi-wall carbon nanotubes on immune and inflammatory responses in mice, J. Toxicol. Sci. 37 (2012) 177–189.
[6] D.W. Porter, A.F. Hubbs, R.R. Mercer, N. Wu, M.G. Wolfarth, K. Sriram, S. Leonard, L. Battelli, D. Schwegler-Berry, S. Friend, M. Andrew, B.T. Chen, S. Tsuruoka, M. Endo, V. Castranova, Mouse pulmonary dose- and time course-responses induced by exposure to multi-walled carbon nanotubes, Toxicology 269 (2010) 136–147.
[7] P. Ravichandran, S. Baluchamy, R. Gopikrishnan, S. Biradar, V. Ramesh, V. Goornavar, R. Thomas, B.L. Wilson, R. Jeffers, J.C. Hall, G.T. Ramesh, Pulmonary biocompatibility assessment of inhaled single-wall and multiwall carbon nanotubes in BALB/c mice, J. Biol. Chem. 286 (2011) 29725–29733.
[8] J.P. Ryman-Rasmussen, M.F. Cesta, A.R. Brody, J.K. Shipley-Phillips, J.I. Everitt, E.W. Tewksbury, O.R. Moss, B.A. Wong, D.E. Dodd, M.E. Andersen, J.C. Bonner, Inhaled carbon nanotubes reach the subpleural tissue in mice, Nat. Nanotechnol. 4 (2009) 747–751.
[9] J. Xu, M. Futakuchi, H. Shimizu, D.B. Alexander, K. Yanagihara, K. Fukamachi, M. Suzui, J. Kanno, A. Hirose, A. Ogata, Y. Sakamoto, D. Nakae, T. Omori, H. Tsuda, Multi-walled carbon nanotubes translocate into the pleural cavity and induce visceral mesothelial proliferation in rats, Cancer Sci. 103 (2012) 2045–2050.
[10] E.J. Park, W.S. Cho, J. Jeong, J. Yi, K. Choi, K. Park, Pro-inflammatory and potential allergic responses resulting from B cell activation in mice treated with multi-walled carbon nanotubes by intratracheal instillation, Toxicology 259 (2009) 113–121.
[11] K. Schroder, J. Tschopp, The inflammasomes, Cell 140 (2010) 821–832.
[12] T. Strowig, J. Henao-Mejia, E. Elinav, R. Flavell, Inflammasomes in health and disease, Nature 481 (2012) 278–286.
[13] E. Meunier, A. Coste, D. Olagnier, H. Authier, L. Lefevre, C. Dardenne, J. Bernad, M. Beraud, E. Flahaut, B. Pipy, Double-walled carbon nanotubes trigger IL-1beta release in human monocytes through Nlrp3 inflammasome activation, Nanomedicine 8 (2012) 987–995.
[14] J. Palomaki, E. Valimaki, J. Sund, M. Vippola, P.A. Clausen, K.A. Jensen, K. Savolainen, S. Matikainen, H. Alenius, Long, needle-like carbon nanotubes and asbestos activate the NLRP3 inflammasome through a similar mechanism, ACS Nano 5 (2011) 6861–6870.
[15] H. Nagai, S. Toyokuni, Biopersistent fiber-induced inflammation and carcinogenesis: lessons learned from asbestos toward safety of fibrous nanomaterials, Arch. Biochem. Biophys. 502 (2010) 1–7.
[16] H. Haniu, Y. Matsuda, K. Takeuchi, Y.A. Kim, T. Hayashi, M. Endo, Proteomics-based safety evaluation of multi-walled carbon nanotubes, Toxicol. Appl. Pharmacol. 242 (2010) 256–262.
[17] M. Pacurari, X.J. Yin, J. Zhao, M. Ding, S.S. Leonard, D. Schwegler-Berry, B.S. Ducatman, D. Sbarra, M.D. Hoover, V. Castranova, V. Vallyathan, Raw single-wall carbon nanotubes induce oxidative stress and activate MAPKs, AP-1, NF-kappaB, and Akt in normal and malignant human mesothelial cells, Environ. Health Perspect. 116 (2008) 1211–1217.

[18] K. Pulskamp, S. Diabate, H.F. Krug, Carbon nanotubes show no sign of acute toxicity but induce intracellular reactive oxygen species in dependence on contaminants, Toxicol. Lett. 168 (2007) 58–74.
[19] V.E. Kagan, Y.Y. Tyurina, V.A. Tyurin, N.V. Konduru, A.I. Potapovich, A.N. Osipov, E.R. Kisin, D. Schwegler-Berry, R. Mercer, V. Castranova, A.A. Shvedova, Direct and indirect effects of single walled carbon nanotubes on RAW 264.7 macrophages: role of iron, Toxicol. Lett. 165 (2006) 88–100.
[20] C. Cheng, K.H. Muller, K.K. Koziol, J.N. Skepper, P.A. Midgley, M.E. Welland, A.E. Porter, Toxicity and imaging of multi-walled carbon nanotubes in human macrophage cells, Biomaterials 30 (2009) 4152–4160.
[21] R. Kato, K. Miyazawa, T. Nishimura, Z.M. Wang, High-resolution transmission electron microscopy of heat-treated C_{60} nanotubes, J. Phys: Conf. Ser. 159 (2009) 012024.
[22] K. Miyazawa, Synthesis and properties of fullerene nanowhiskers and fullerene nanotubes, J. Nanosci. Nanotechnol. 9 (2009) 41–50.
[23] K. Miyazawa, Y. Kuwasaki, A. Obayashi, M. Kuwabara, C_{60} nanowhiskers formed by the liquid–liquid interfacial precipitation method, J. Mater. Res. 17 (2002) 83–88.
[24] H. Nagai, Y. Okazaki, S.H. Chew, N. Misawa, Y. Yamashita, S. Akatsuka, T. Ishihara, K. Yamashita, Y. Yoshikawa, H. Yasui, L. Jiang, H. Ohara, T. Takahashi, G. Ichihara, K. Kostarelos, Y. Miyata, H. Shinohara, S. Toyokuni, Diameter and rigidity of multiwalled carbon nanotubes are critical factors in mesothelial injury and carcinogenesis, Proc. Natl. Acad. Sci. U.S.A. 108 (2011) E1330–E1338.
[25] P. Haberzettl, R. Duffin, U. Kramer, D. Hohr, R.P. Schins, P.J. Borm, C. Albrecht, Actin plays a crucial role in the phagocytosis and biological response to respirable quartz particles in macrophages, Arch. Toxicol. 81 (2007) 459–470.
[26] C. Dostert, V. Petrilli, B.R. Van, C. Steele, B.T. Mossman, J. Tschopp, Innate immune activation through Nalp3 inflammasome sensing of asbestos and silica, Science 320 (2008) 674–677.
[27] A. Rubartelli, Redox control of NLRP3 inflammasome activation in health and disease, J. Leukoc. Biol. 92 (2012) 951–958.
[28] M.T. Heneka, M.P. Kummer, A. Stutz, A. Delekate, S. Schwartz, A. Vieira-Saecker, A. Griep, D. Axt, A. Remus, T.C. Tzeng, E. Gelpi, A. Halle, M. Korte, E. Latz, D.T. Golenbock, NLRP3 is activated in Alzheimer's disease and contributes to pathology in APP/PS1 mice, Nature 493 (2013) 674–678.